Supporting Information

Cyclic Voltammetry Driven Bi–Ag Single-Atom Alloy Electrocatalysts for Enhanced CO_2-to-Formate Conversion

Yongsu An[a], Sunglun Kwon[b], Young Heon Kim[c], Chan Woo Lee[d, *], Duk-Young Jung[a, *]

[a]Department of Chemistry, Sungkyun Advanced Institute of Nanotechnology (SAINT), Sungkyunkwan University, Suwon, 16419, Republic of Korea

[b]Department of Chemistry, The Catholic University of Korea, Bucheon, 14662, Republic of Korea

[c]Graduate School of Analytical Science and Technology (GRAST), Chungnam National University, Daejeon, 34134, Republic of Korea

[d]Department of Chemistry, Kookmin University, Seoul, 02707, Republic of Korea

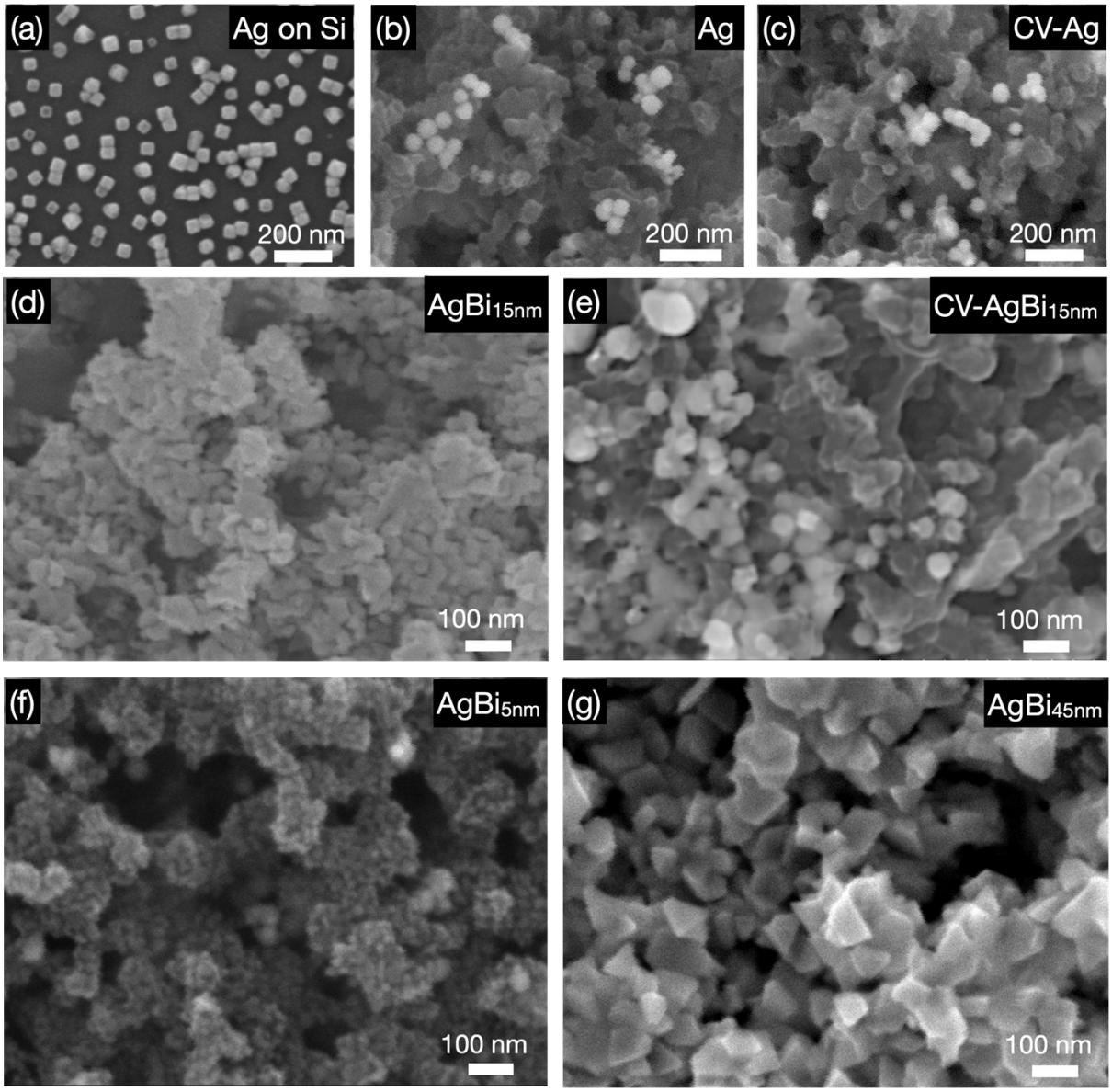

Fig. S1. SEM image of (a) Ag nanoparticles on Si wafer, (b) Ag on carbon paper (Ag), (c) CV treated Ag on carbon paper (CV-Ag), (d) Bi 15 nm layer on Ag ($AgBi_{15nm}$), (e) CV treated Bi 15 nm layer on Ag (CV-$AgBi_{15nm}$), (f) Bi 5 nm and (g) Bi 45 nm layer on Ag ($AgBi_{5nm}$ and $AgBi_{45nm}$), respectively.

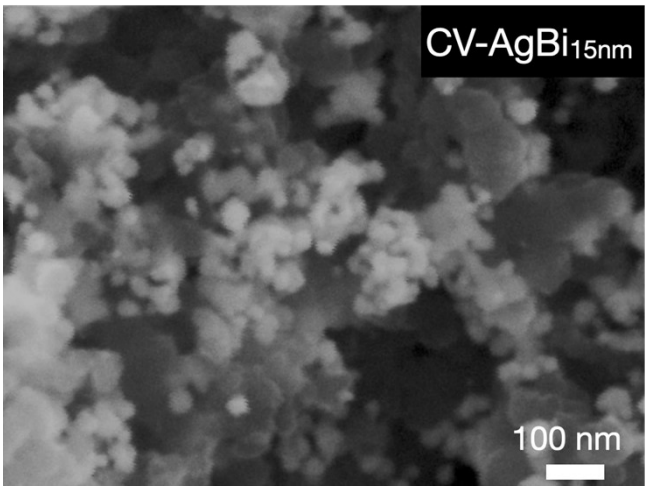

Fig. S2. SEM image of CV treated Bi 15 nm layer on Ag (CV-$AgBi_{15nm}$) after 1 hour of CO_2RR.

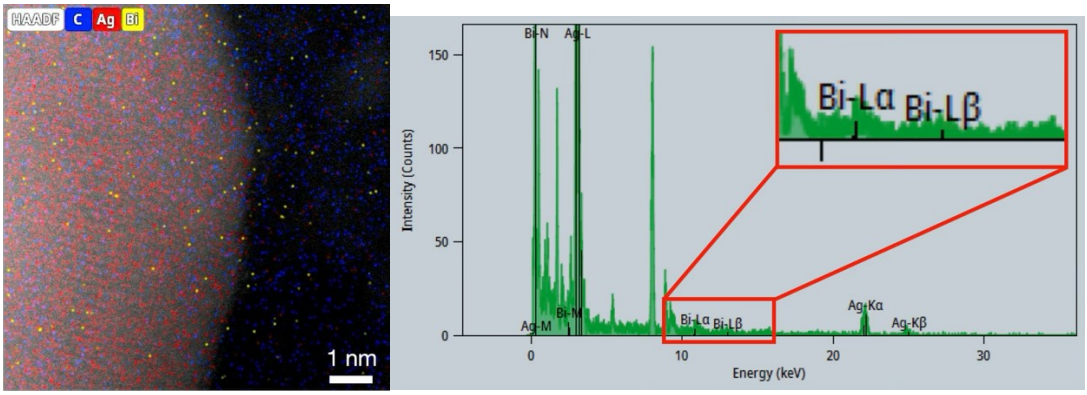

Fig. S3. HAADF-STEM-EDS spectrum of CV-$AgBi_{15nm}$.

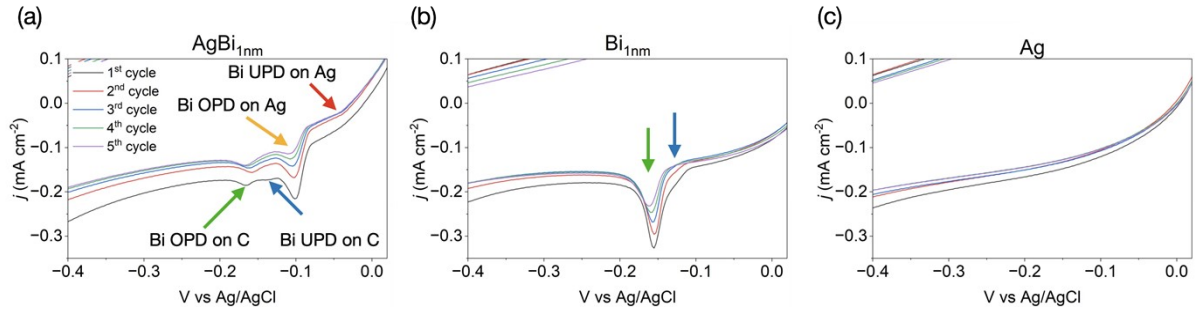

Fig. S4. Cyclic voltammetry curves of (a) $AgBi_{1nm}$, (b) Bi_{1nm} and (c) Ag, scanned from -0.9 to 0.08 V.

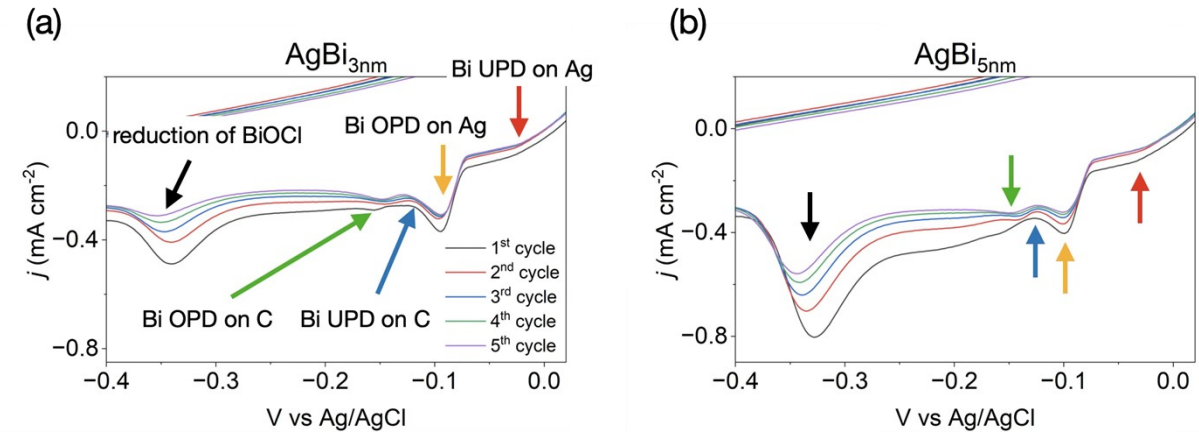

Fig. S5. Cyclic voltammetry curves of $AgBi_{3nm}$ and $AgBi_{5nm}$, scanned from -0.9 to 0.08 V.

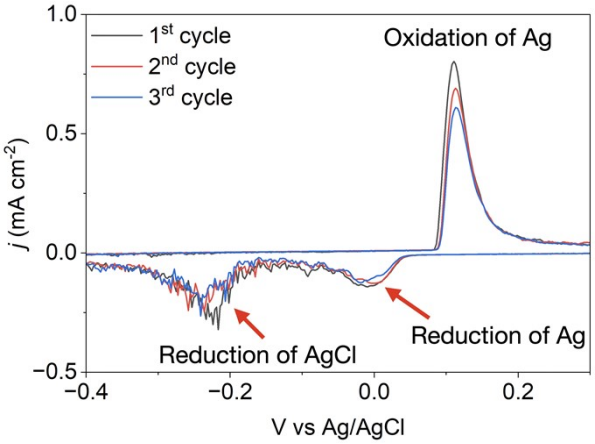

Fig. S6. Cyclic voltammetry curve of Ag, scanned from -0.9 to 0.5 V.

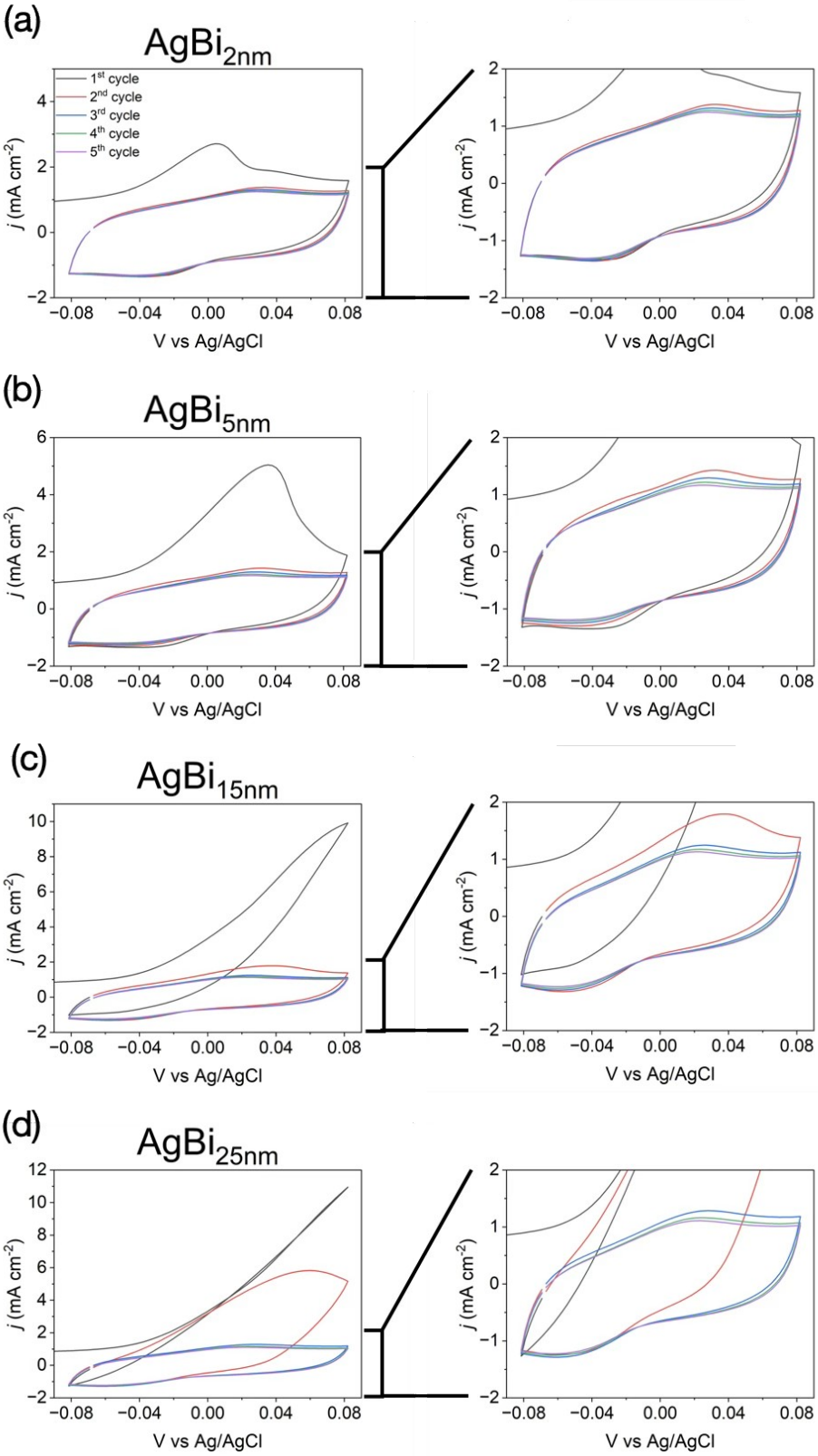
(a)
AgBi2nm
1st cycle
2nd cycle
3rd cycle
4th cycle
5th cycle
j (mA cm-2)
V vs Ag/AgCl
(b)
AgBi5nm
(c)
AgBi15nm
(d)
AgBi25nm

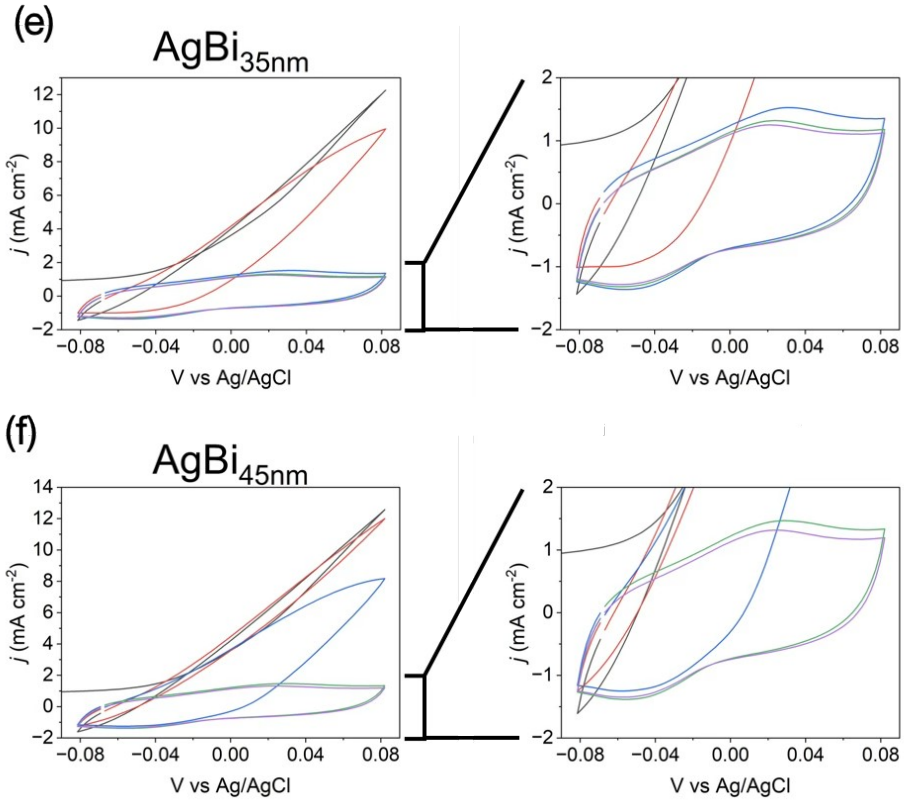

Fig. S7. Cyclic voltammetry curves and their magnified Figures of (a) $AgBi_{2nm}$, (b) $AgBi_{5nm}$, (c) $AgBi_{15nm}$, (d) $AgBi_{25nm}$, (e) $AgBi_{35nm}$ and (f) $AgBi_{45nm}$, respectively.

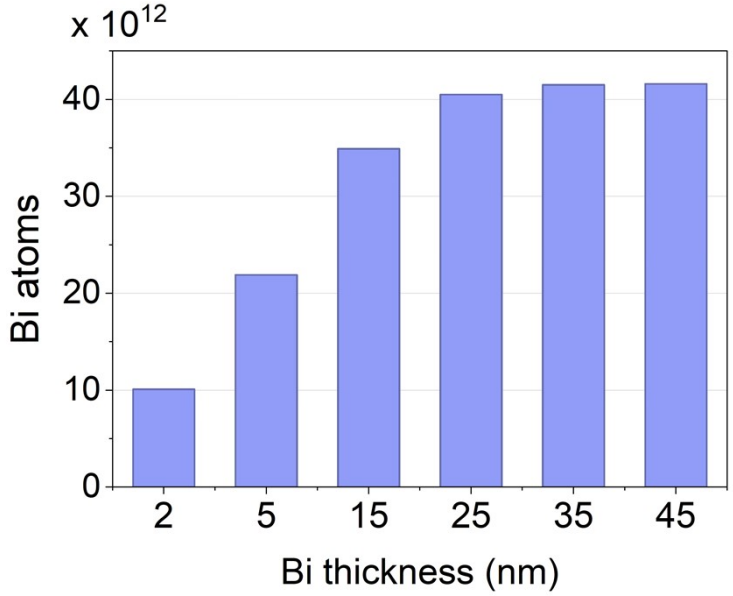

Fig. S8. The number of reduced Bi atoms on Ag calculated form the reduction peak of cyclic voltammetry curve.

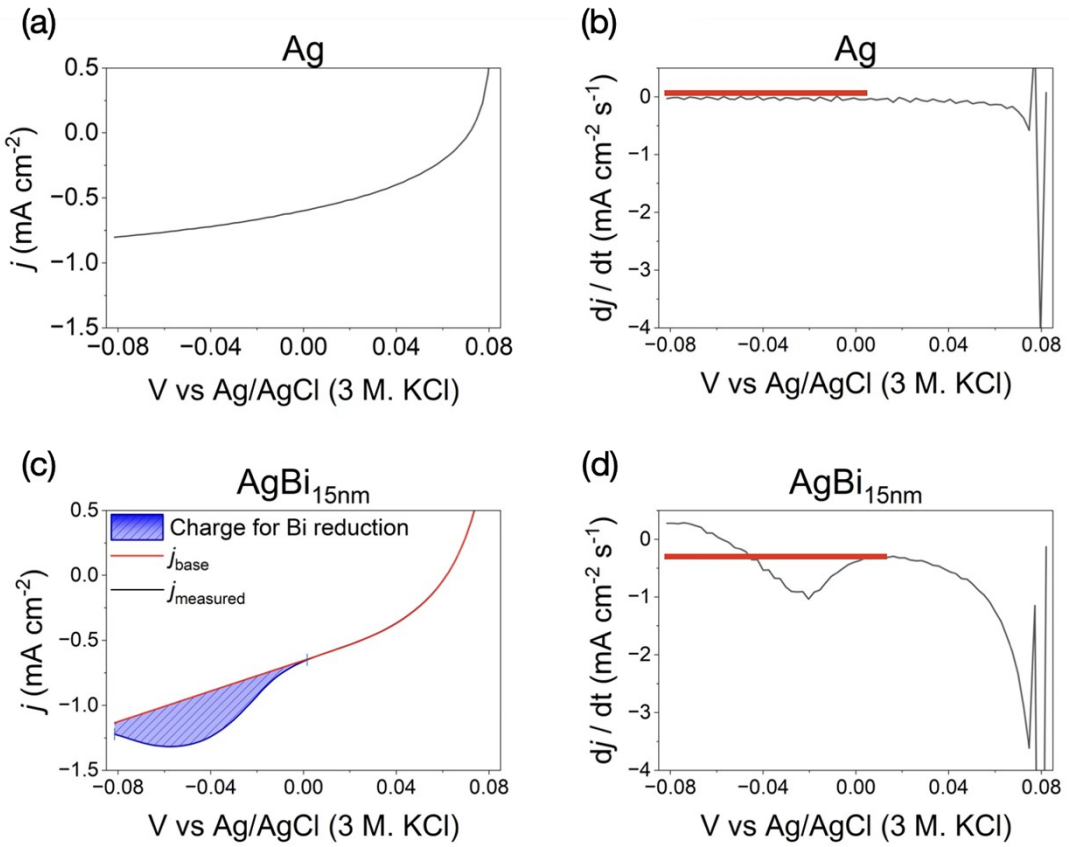

Fig. S9. Calculation of the amount of reduced Bi atoms from cyclic voltammetry curves.

Quantification of reduced Bi from CV (Fig. S8)

The amount of reduced Bi was calculated from the cyclic voltammetry curves (Fig. S8) by differentiating the current density (j) with respect to time and by reconstructing an Ag-like baseline. Direct substraction of the Ag curve as a baseline was not adopted because current densities vary across samples and can't be completely fitted. In contrast, dj/dt for Ag was essentially constant for V ≤ 0 V (Fig. S8b), whereas the onset of Bi reduction in AgBi occurred at approximately 0 V. Accordingly, by setting values of dj/dt under 0 V equal to its value at V = 0 V, the dj/dt curve of AgBi was constrained to an Ag-like constant, yielding the Ag-like dj/dt profile shown in Fig. S8d. And then, integration of this constrained dj/dt yielded the reconstructed baseline j_{base} (red line in Fig. S8c). The Bi reduction current was then obtained as $j_{measured}$ - j_{base}, and the corresponding charge (blue-shaded area) as

$$Q_{Bi} = \frac{1}{\nu} \int_{-0.08}^{0} [j_{measured} - j_{base}] dV$$

$$n_{Bi} = Q_{Bi}/(3F)$$

With ν = 50 mV s^{-1}.

Based on the number of scans required for complete removal of Bi on carbon, the integration was carried out over 1st cycle for $AgBi_{2nm}$ and $AgBi_{5nm}$, 2nd cycle for $AgBi_{15nm}$ and $AgBi_{25nm}$, and 3rd cycle for $AgBi_{35nm}$ and $AgBi_{45nm}$.

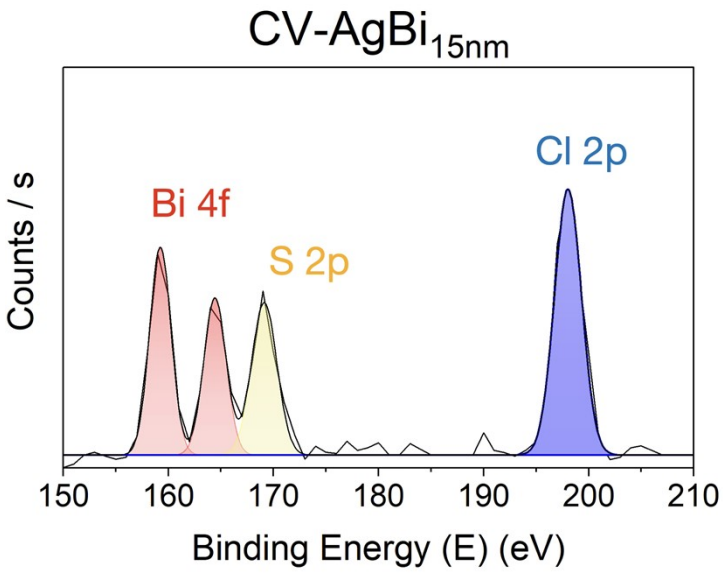

atomic ratio (%)	
Bi 4f	17.5
Cl 2p	82.5

Fig. S10. Comparison of atomic ratio of Bi and Cl in CV-$AgBi_{15nm}$ based on the full scan XPS data.

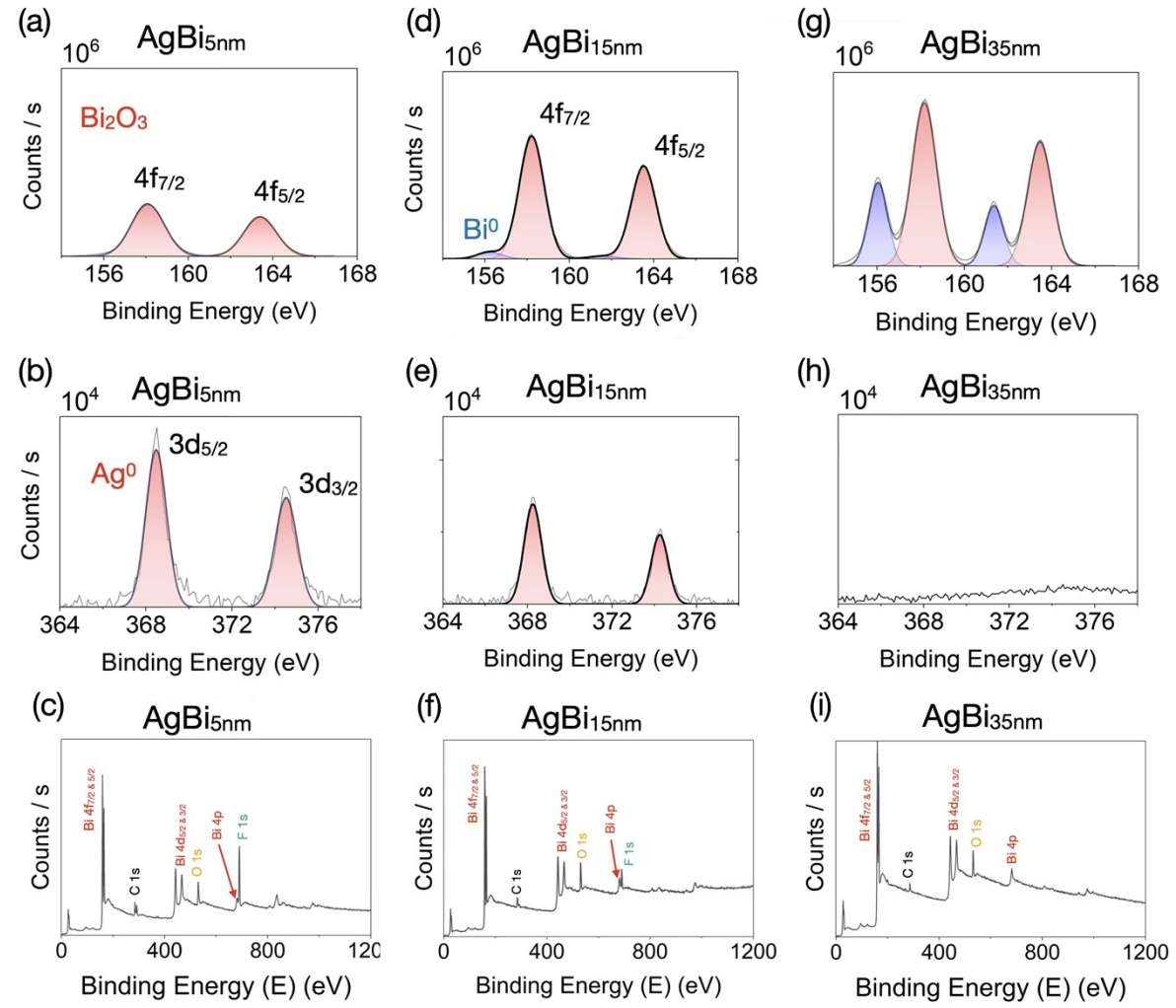

Fig. S11. XPS spectra of $AgBi_{5nm}$ (a–c), $AgBi_{15nm}$ (d–f) and $AgBi_{35nm}$ (g–i). Spectra are shown for (a, d, g) Bi 4f, (b, e, h) Ag 3d, and (c, f, i) full scan, respectively.

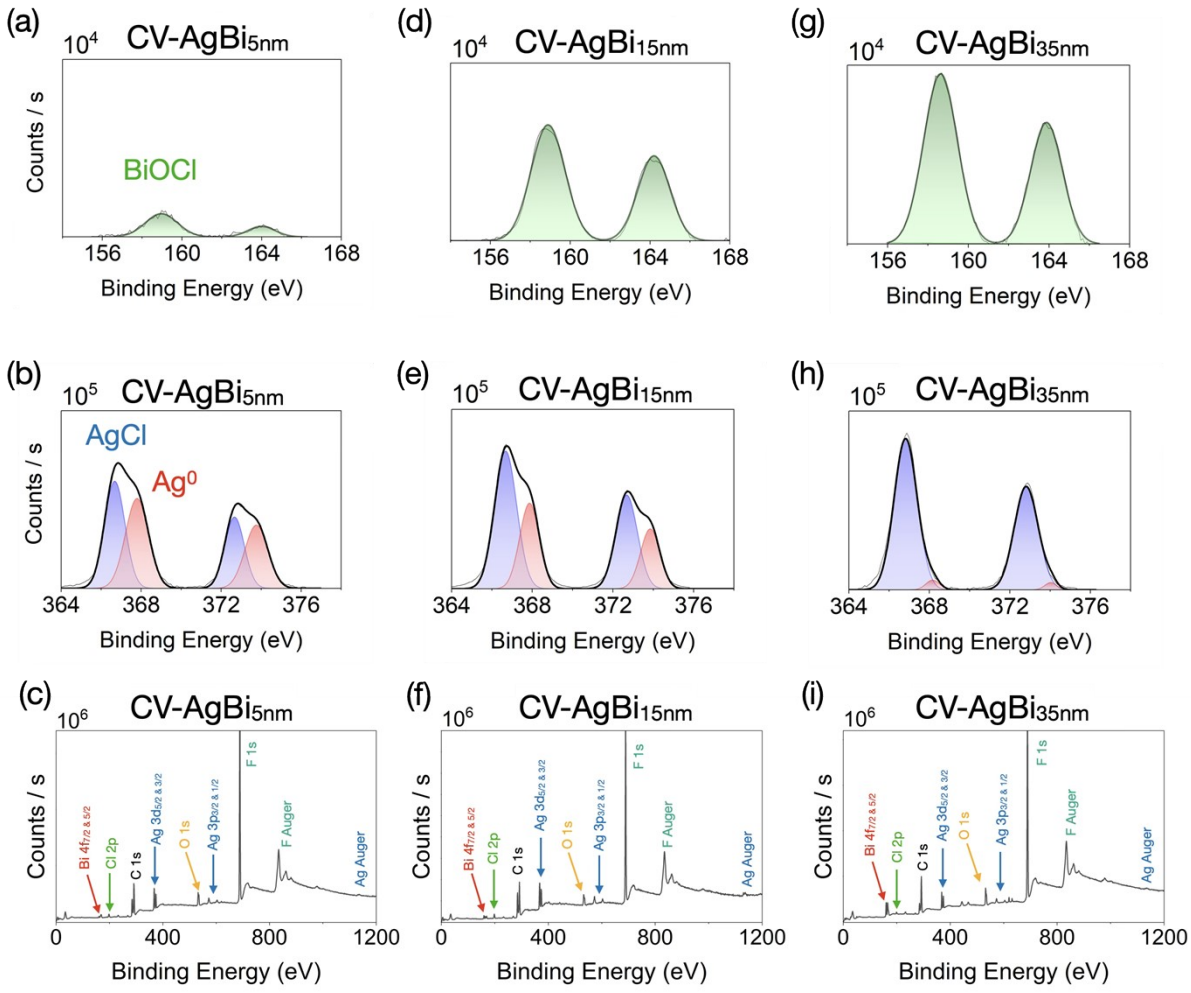

Fig. S12. XPS spectra of CV-$AgBi_{5nm}$ (a–c), CV-$AgBi_{15nm}$ (d–f) and CV-$AgBi_{35nm}$ (g–i). Spectra are shown for (a, d, g) Bi 4f, (b, e, h) Ag 3d, and (c, f, i) full scan, respectively.

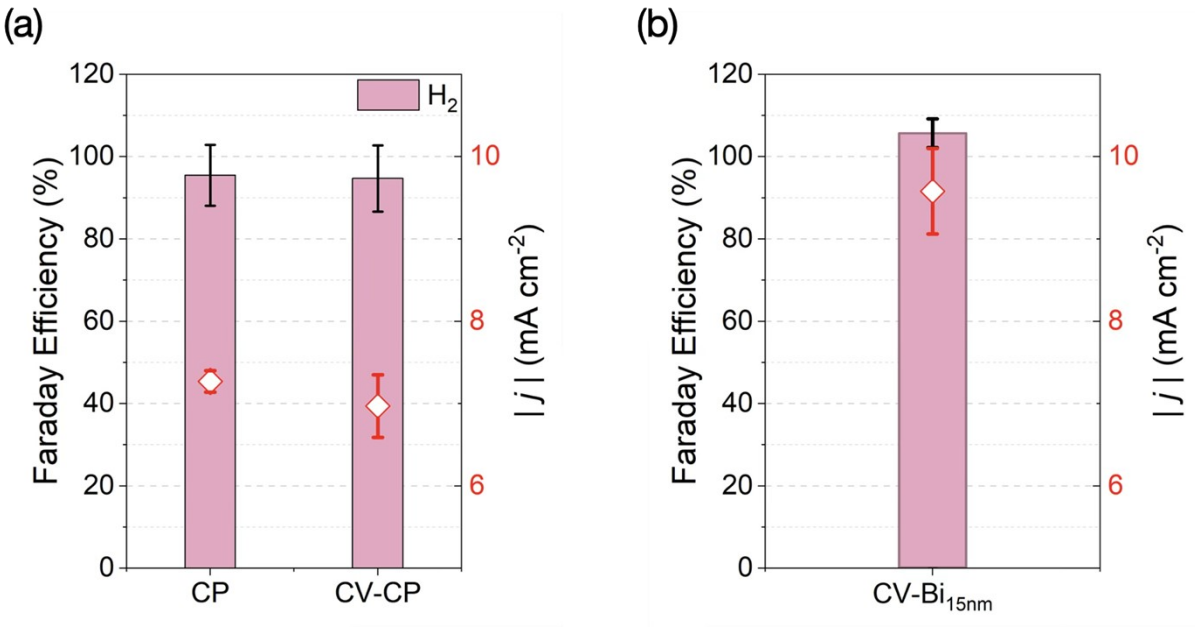

Fig. S13. Faraday efficiency of (a) CP and CV-CP, and of CV-Bi_{15nm}.

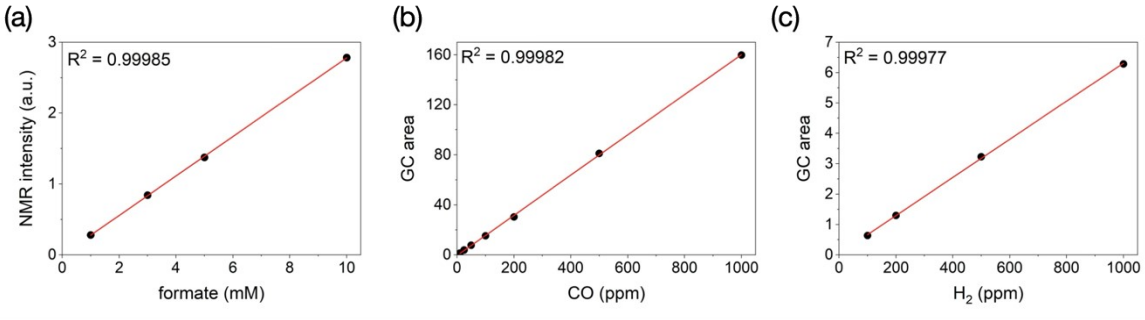

Fig. S14. Calibration curves for quantitative analysis. (a) The calibration curve of $HCOO^-$ is obtained by plotting the relative area of $HCOO^-$ signal of standard samples containing 1, 3, 5, 10 mM of $HCOO^-$. The calibration curves of (b) CO and (c) H_2 are obtained by plotting the area of standard gases containing 10, 25, 50, 100, 200, 500, 1000 ppm of CO and 100, 200, 500, 1000 ppm of H_2, respectively.

Element	$AgBi_{15nm}$	Binding Energy (eV)	CV-$AgBi_{15nm}$	Binding Energy (eV)
Ag	Ag^0 $3d_{5/2}$	368.2	Ag^0 $3d_{5/2}$	367.9
	Ag^0 $3d_{3/2}$	374.3	Ag^0 $3d_{3/2}$	373.8
			AgCl $3d_{5/2}$	366.7
			AgCl $3d_{3/2}$	372.7
Bi			BiOCl $4f_{7/2}$	158.9
			BiOCl $4f_{5/2}$	164.2
	Bi_2O_3 $4f_{7/2}$	158.2		
	Bi_2O_3 $4f_{5/2}$	163.5		
	Bi^0 $4f_{7/2}$	156.2		
	Bi^0 $4f_{5/2}$	161.6		
O	O1	529.5		
	O2	530.5		
	C-O bonds	531.9	C-O bonds	531.7
			Nafion	534.7

Table S1. Binding energy of each elements of AgBi samples from XPS data (O1 is from non-defective metal oxide and O2 is from defective metal oxide).

JCPDS	peak
Ag (111) #2-1098	38.28º
$Ag_{99.5}Bi_{0.5}$ (111) # 65-8426	38.14º
Bi (104) #44-1246	37.95º

Table S2. reference XRD peak from JCPDS.